π Groups in Ion Pair Bonding. The Effect of the Cation on the Structural and Spectroscopic Properties of Fluorenyl Ion Pairs

R. Zerger, W. Rhine, and G. D. Stucky*

Contribution from the School of Chemical Sciences and Materials Research Laboratory, University of Illinois, Urbana, Illinois 61801. Received February 9, 1974

Abstract: The synthesis and isolation of the 1:1 complexes of fluorenyllithium with pentamethyldiethylenetriamine and hexamethylphosphoramide, the 1:1 complex of fluorenylpotassium with tetramethylethylenediamine, the 1:2 complex of fluorenyllithium with tetrahydrofuran, and the unsolvated fluorenyltetra(n-propyl)ammonium salt are described. The visible absorption spectra of these compounds were examined in order to determine the effects of solvation number and cation position on the 340–380 nm band in the fluorenyl carbanion. A comparison of the solid state and solution spectra is given. In addition, the molecular and crystal structure of fluorenylpotassium tetramethylethylenediamine (FlK–TMEDA), $C_{13}H_9K(N_2C_6H_{16})$, was determined from single-crystal X-ray data (2785 reflections) measured on a four-circle Picker X-ray diffractometer equipped with a graphite monochromator. The crystal system is monoclinic with $a = 10,000 (6)$ Å, $b = 17.425 (12)$ Å, $c = 11.080 (8)$ Å, and $\beta = 108.71 (3)°$, four molecules of $C_{13}H_9K(N_2C_6H_{16})$ per unit cell, and $\rho_{calcd} = 1.164$ g cm^{-3}. Least-squares refinement gave a final agreement factor of $R_w = 0.044$ and $R = 0.043$. The tetramethylethylenediamine group is not bidentate but instead bridges two potassium atoms. Each potassium atom is associated with two nitrogen atoms and two fluorenyl groups with a potassium ring plane distance of 3.052 (1) and 2.972 (1) Å. The nitrogen–potassium–nitrogen atom angle is 90.4 (1)°. The geometry of the fluorenyl carbanion agrees well with that predicted by simple molecular orbital calculations.

It is now generally accepted that many of the solution properties of unsaturated alkali metal organometallic compounds can be interpreted in terms of two distinct species which may coexist in a rapid equilibrium.[1]

$$R^-M^+ + nS \rightleftharpoons R^-||M^+ \quad (1)$$

(S = solvent molecule of solvation)

The distinguishing feature of the two ion pairs, R^-M^+ and $R^-||M^+$ is presumably a change in the degree of solvation of M^+.

Some information as to what one might expect for the coordination of the metal to the delocalized carbanion for species such as R^-M^+ was recently reported in a series of studies on the solid state molecular structures of disolvated lithium complexes: benzyl-,[2] fluorenyl-,[3] and triphenylmethyllithium.[4] It was noted that the detailed molecular structures of these solvated ion pairs could not be predicted solely by electrostatic considera-

tions but that they were consistent with some directed covalent interaction involving the formation of a three-center bond between an unoccupied lithium orbital and the highest occupied molecular orbital of the carbanion. It was also suggested that, for these carbanions, the position of an alkali metal with respect to the carbanion could be expected to be dependent on the degree of solvation and atomic number of the metal; e.g., a position directly over the five-membered ring of the fluorenyl carbanion was predicted for the heavier alkali metals or for trisolvated lithium. This could result in the possibility of solution equilibria for fluorenyllithium of the form

$$S_2LiF + S \rightleftharpoons S_3LiFl \quad (2)$$

$$S_3LiF + S \rightleftharpoons S_4Li^+ Fl^- $$
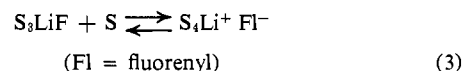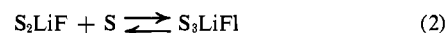
(Fl = fluorenyl) $\quad (3)$

In the eq 2, the position of the lithium atom with respect to the fluorenyl group may be altered as indicated above.

The nature of the cation-coordinated base interaction is also of importance in understanding the properties of ion pairs. For example, the physical properties of the very important N,N,N',N'-tetramethylethylenediamine

(1) See, for example, T. E. Hogen-Esch and J. Smid, *J. Amer. Chem. Soc.*, **87**, 669 (1965); **88**, 307, 318 (1966).

(2) S. P. Patterman, I. L. Karle, and G. D. Stucky, *J. Amer. Chem. Soc.*, **92**, 1150 (1970).

(3) J. J. Brooks, W. Rhine, and G. D. Stucky, *J. Amer. Chem. Soc.*, **94**, 7339 (1972).

(4) J. J. Brooks and G. D. Stucky, *J. Amer. Chem. Soc.*, **94**, 7333 (1972).

(TMEDA) complexes of organolithium reagents are quite different from those of TMEDA complexes of the heavier alkali metals. Thus, fluorenylpotassium–TMEDA is much less soluble than fluorenyllithium–TMEDA in solvents such as benzene. This is of obvious importance to the utilization of the heavier alkali metal organometallic compounds as chemical reagents and as homogeneous polymerization catalysts. A study of the stereochemical properties of FlK–TMEDA could be expected to lead to a much clearer understanding of the role of both the coordinating base and the metal–carbanion interaction in metal–carbanion chemistry.

Much of the interpretation of the structure of ion pairs in solution is based on optical spectroscopic data. The fluorenyl carbanion is particularly well-suited for these studies since in solution it has a well-resolved absorption band at 345–375 nm ($\epsilon \sim 10{,}000$), which is sensitive to variations in the nature of the anion–cation interaction. An important question is whether or not solid state spectroscopic data for the fluorenyl carbanion can be related to solution data. For example, what happens to the 345–375 nm band in the solid state spectra of the fluorenyl carbanion systems? How much, if any, has it shifted relative to the solution spectra and is it still sensitive to changes in the cation–anion interaction? If these questions could be answered, it should be possible to determine the relation, if any, of R^-M^+ and $R^-\|M^+$ in eq 1 to the various components of eq 2 and 3. In this paper, some preliminary observations concerning this point are presented.

Experimental Section

A. Syntheses. Fluorenyllithium was prepared by treating 1.03 g (6.25 mmol) of fluorene with 6.25 mmol of n-butyllithium in approximately 150 ml of benzene under a nitrogen atmosphere. The resulting yellow-orange solution was then taken into an argon filled drybox and heated and filtered. The solution, after a few hours, yielded a yellow crystalline solid.

The solvated fluorenyllithium complexes were prepared by treating 6.25 mmol of n-butyllithium with 1.03 g (6.25 mmol) of fluorene in about 150 ml of benzene. To this solution was added the appropriate molar amount of the desired coordinating base. The resulting solutions were then taken into an argon filled drybox and filtered. On standing with partial evaporation of the solvent, the solutions yielded the desired complexes. Yields were in all cases greater than 90%. After recrystallization, the samples were dissolved in benzene and characterized by their nmr spectra.

The tetra-n-propylammonium salt of fluorene was prepared by the addition of an equimolar amount of tetra-n-propylammonium bromide to a previously prepared solution of fluorenyllithium. The resulting solution was then filtered in a drybox and the solvent was evaporated yielding large dark orange crystals.

Fluorenylpotassium was prepared in a manner similar to that described by Scherf.[5] A 4.12 g (0.025 mol) sample of fluorene was dissolved in 60 ml of dry dioxane in a round-bottom flask which had been flushed with N_2 gas and fitted with a reflux condenser. Under a nitrogen atmosphere 0.98 g (0.025 mol) of potassium metal was added, and the mixture was refluxed. After 2 hr, all the potassium had reacted and the dark yellow-orange solution was cooled. The solution was then taken into a helium filled drybox and filtered yielding a reddish brown powder. The powder was then dissolved in a hot benzene–N,N,N',N'-tetramethylethylenediamine (TMEDA) mixture. Evaporation of the solvent yielded dark orange crystals which were not suitable for X-ray analysis. The crystals were redissolved in a 50–50 mixture of benzene, and TMEDA and the solution was allowed to evaporate overnight. This solution gave very large dark orange prisms which were cleaved to a suitable size for X-ray analysis.

B. Solid State Spectroscopic Characterization. The samples for the ultraviolet and visible spectra were prepared in an argon filled drybox. The Nujol used in the preparation of the samples was dried over sodium and stored in the drybox. Precautions such as greasing the edges of the quartz plates containing the sample were taken to minimize decomposition of the sample. Very little, if any, decomposition took place even after the samples had remained in the air for several hours.

C. X-Ray Analysis. 1. Data Collection and Reduction. $C_{13}H_9K(N_2C_6H_{16})$ is very sensitive to oxygen and water. Therefore, the crystals used for X-ray analysis were cleaved as necessary to the proper size and sealed in thin-walled glass capillaries.

Preliminary precession photographs showed the crystals to be monoclinic with systematic absences on $h0l$ for $l = 2n + 1$, and on $0k0$ for $k = 2n + 1$. These absences uniquely determined the space group $P2_1/c$. A suitable crystal was chosen which had the shape of a triangular prism with sides of 0.28, 0.30, and 0.35 mm and with a length of 0.50 mm. The crystal was mounted so that the rotation axis was coincident with the a^* axis.

Twelve reflections were carefully centered on a Picker four-circle diffractometer and used in a least-squares refinement of the lattice parameters ($T = 23°$, λ 0.71069 Å). The cell constants obtained were $a = 10.000$ (6) Å, $b = 17.425$ (12) Å, $c = 11.080$ (8) Å, and $\beta = 108.71$ (3)°.

Due to the reactivity of the crystals with the halogenated hydrocarbons used for the density measurements by the flotation method, an accurate density measurement was not obtained. A density of 1.164 cm^{-3} was calculated assuming four asymmetric units of $C_{13}H_9K(N_2C_6H_{16})$ per unit cell. This is a reasonable density considering the fact that the density for fluorenyllithium bisquinuclidine[3] is 1.15 g cm^{-3}.

Diffraction data were collected on a fully automated Picker four-circle diffractometer equipped with a highly oriented graphite single crystal monochromator using Mo Kα radiation. Data were measured using the θ–2θ scan technique with a scan rate of 1.0°/min and a scan width of 1.5°. Stationary crystal–stationary counter background counts of 10 sec were taken at the beginning and at the end of each scan. A takeoff angle of 2.15° gave approximately 80% of the intensity of a typically large peak. Pulse height analyzer settings of 3.0 and 8.0 for the lower and upper level discriminators, respectively, were used. Several ω scans showed the typical full peak width at half height to be less than 0.14° indicating that the mosaicity was acceptably low for data collection. Copper foil attenuators whose attenuation factors were known were automatically inserted in front of the counter aperture whenever the counting rate exceeded 10,000 counts per second in order to eliminate saturation of the counter circuit. Three standard peaks were monitored every 60 reflections to ensure crystal and counter stability. Because of mechanical problems with the diffractometer, the crystal had to be recentered several times during the course of data collection. After these corrections were made, the standard reflections showed no systematic change in intensity throughout data collection.

A full form of data (hkl and $\bar{h}kl$) was measured to $2\theta_{max} = 45°$ resulting in 2785 reflections of which 2257 were unique. The intensities were corrected for background and Lorentz and polarization factors, and structure factor amplitudes were calculated using a local computer program, GORDO. Due to the relatively small linear absorption coefficient ($\mu = 2.88$ cm^{-1}) and the prismatic shape of the crystal, no absorption correction was made. Of the unique data, 1258 reflections were considered observed using the criteria $I_{obsd} \geq 3\sigma_c(I)$ where

$$\sigma_c = [T_c + 0.25(t_c/t_b)^2(B_1 + B_2)]^{1/2}$$

T_c is the total integrated counts, t_c/t_b is the ratio of the time spent counting the peak intensity to the time spent counting the background intensities and B_1 and B_2 are background counts.

2. Solution and Refinement of the Structure. The solution of the structure was obtained by the symbolic addition procedure using the program MULTAN.[6]

The scattering factors used in the refinement for C^0, N^0, and K^0 were taken from the compilation of Hanson, et al.,[7] and those for

---

(5) G. W. H. Scherf and R. K. Brown, *Can. J. Chem.*, 38, 697 (1960).

(6) G. Germain, P. Main, and M. M. Woolfson, *Acta Crystallogr.*, *Sect. B*, 26, 274 (1970).

(7) H. P. Hanson, F. Herman, J. D. Lee, and S. Skillman, *Acta Crystallogr.*, 17, 1040 (1964).

Table I. Positional Parameters for the Non-Hydrogen Atoms in $C_{13}H_9K(N_2C_6H_{16})$

Atom	x	y	z
C(1)	0.1823 (4)	0.2760 (2)	0.0511 (3)
C(2)	0.0836 (4)	0.2332 (3)	−0.0344 (4)
C(3)	0.1178 (4)	0.1742 (2)	−0.1041 (3)
C(4)	0.2572 (4)	0.1577 (2)	−0.0844 (3)
C(5)	0.6091 (4)	0.1507 (2)	0.0059 (3)
C(6)	0.7508 (4)	0.1650 (2)	0.0533 (4)
C(7)	0.8026 (3)	0.2212 (2)	0.1449 (4)
C(8)	0.7153 (4)	0.2671 (2)	0.1848 (3)
C(9)	0.4505 (4)	0.2962 (2)	0.1501 (3)
C(10)	0.3266 (4)	0.2615 (2)	0.0719 (3)
C(11)	0.3640 (4)	0.2005 (2)	0.0042 (3)
C(12)	0.5134 (3)	0.1976 (2)	0.0418 (3)
C(13)	0.5670 (4)	0.2575 (2)	0.1330 (3)
N(1)	0.2575 (3)	0.0490 (2)	0.2823 (3)
N(2)	0.3011 (3)	−0.0562 (2)	0.5889 (3)
AC(1)	0.2606 (5)	0.0109 (2)	0.1667 (5)
AC(2)	0.1365 (5)	0.0989 (2)	0.2510 (4)
AC(3)	0.2525 (4)	−0.0110 (3)	0.3697 (5)
AC(4)	0.2792 (5)	0.0041 (3)	0.4960 (4)
AC(5)	0.1819 (5)	−0.1071 (2)	0.5627 (4)
AC(6)	0.3199 (5)	−0.0179 (2)	0.7084 (4)
K	0.4688 (1)	0.1715 (1)	0.3510 (1)

refinement, all 2257 unique reflections were included in the refinement with counting statistical weights

$$\sigma(F) = \frac{F}{2I}\left[T_c + 0.25\left(\frac{t_c}{t_b}\right)^2(B_1 + B_2) + (KI)^2\right]^{1/2}, \quad K = 0.02$$

In addition, all negative F_{obsd} were set equal to zero. After six additional cycles of full anisotropic refinement of the non-hydrogen atoms and several separate cycles of refinement of the hydrogen atom positions and isotropic temperature factors, the R factors converged at

$$R_1 = \sum|F_o - F_c|/\sum|F_o| = 0.043$$

$$R_2 = 0.044$$

The estimated standard deviation of an observation of unit weight

$$(ERF) = [\sum\omega(F_o - F_c)^2/(NO - NV)]^{1/2}$$

where NO is the number of observations and NV is the number of variables was 1.51. A final difference Fourier map showed no peaks of greater than 0.446 e/Å³. A test of the counting statistics weighting scheme showed no systematic variation of $\omega(F_o - F_c)^2$ with the magnitude of the structure factors or with increasing sin θ/λ. Due to a rather small core storage, it was necessary to vary

Table II. Anisotropic Thermal Parameters for the Non-Hydrogen Atoms in $C_{13}H_9K(N_2C_6H_{16})$

Atom	$\beta_{11}{}^a$	β_{22}	β_{33}	β_{12}	β_{13}	β_{23}
C(1)	0.0156 (6)	0.0051 (2)	0.0131 (5)	0.0026 (3)	0.0061 (4)	0.0008 (2)
C(2)	0.0105 (6)	0.0075 (2)	0.0153 (5)	0.0010 (3)	0.0043 (5)	0.0028 (3)
C(3)	0.0155 (7)	0.0066 (2)	0.0143 (5)	−0.0003 (3)	0.0030 (5)	−0.0013 (3)
C(4)	0.0162 (6)	0.0052 (2)	0.0120 (4)	0.0010 (3)	0.0041 (4)	−0.0004 (2)
C(5)	0.0147 (6)	0.0051 (2)	0.0107 (4)	0.0004 (3)	0.0030 (4)	−0.0008 (2)
C(6)	0.0151 (6)	0.0069 (2)	0.0133 (5)	0.0014 (3)	0.0056 (4)	−0.0007 (3)
C(7)	0.0109 (5)	0.0066 (2)	0.0137 (5)	0.0002 (3)	0.0029 (4)	0.0012 (3)
C(8)	0.0154 (6)	0.0044 (2)	0.0107 (4)	−0.0005 (3)	0.0024 (4)	0.0003 (2)
C(9)	0.0175 (6)	0.0032 (1)	0.0103 (4)	0.0006 (2)	0.0036 (4)	−0.0004 (2)
C(10)	0.0135 (6)	0.0037 (1)	0.0092 (4)	0.0012 (2)	0.0045 (4)	0.0009 (2)
C(11)	0.0135 (6)	0.0037 (1)	0.0081 (4)	0.0000 (2)	0.0031 (4)	0.0002 (2)
C(12)	0.0122 (5)	0.0038 (1)	0.0083 (4)	0.0013 (2)	0.0035 (4)	0.0008 (2)
C(13)	0.0132 (5)	0.0036 (1)	0.0084 (4)	0.0002 (2)	0.0030 (4)	0.0012 (2)
N(1)	0.0241 (6)	0.0044 (1)	0.0132 (4)	0.0014 (2)	0.0079 (4)	0.0017 (2)
N(2)	0.0257 (6)	0.0043 (1)	0.0133 (4)	−0.0016 (2)	0.0088 (4)	0.0011 (2)
AC(1)	0.0418 (11)	0.0075 (2)	0.0241 (7)	0.0025 (4)	0.0126 (7)	−0.0015 (3)
AC(2)	0.0345 (9)	0.0076 (2)	0.0204 (6)	0.0059 (4)	0.0093 (6)	0.0011 (3)
AC(3)	0.0241 (8)	0.0089 (3)	0.0206 (7)	−0.0035 (4)	0.0014 (6)	0.0035 (4)
AC(4)	0.0438 (12)	0.0111 (3)	0.0139 (6)	−0.0124 (5)	0.0017 (7)	0.0017 (4)
AC(5)	0.0351 (9)	0.0065 (2)	0.0219 (6)	−0.0039 (4)	0.0143 (7)	0.0011 (3)
AC(6)	0.0446 (11)	0.0066 (2)	0.0192 (6)	−0.0024 (4)	0.0111 (7)	−0.0015 (3)
K	0.0284 (2)	0.0035 (1)	0.0146 (1)	0.0003 (1)	0.0090 (1)	−0.0001 (1)

^{a} The form of the anisotropic ellipsoid is $\exp[-(\beta_{11}h^2 + \beta_{22}k^2 + \beta_{33}l^2 + 2\beta_{12}hk + 2\beta_{13}hl + 2\beta_{23}kl)]$.

the hydrogen atom are the best spherical form factors of Stewart, et al.[8] All calculations were carried out on an XDS Sigma 5 computer.

Isotropic refinement on all non-hydrogen atoms converged at

$$R_2 = (\sum\omega(F_o - F_c)^2/\sum\omega F_o^2)^{1/2} = 0.139$$

The theoretical positions for the hydrogen atoms were calculated using a local computer program HYGEN. Each hydrogen atom was placed in the calculated position 1.02 Å from its parent carbon atom and given an isotropic thermal parameter equal to the converged isotropic thermal parameter of that carbon atom. When the hydrogen atoms were included in the refinement, the value of R_2 dropped to 0.113. Anisotropic temperature factors were then used for the non-hydrogen atoms and six cycles of refinement gave a value of $R_2 = 0.048$. Up to this point, unit weights and 1478 reflections with $I_{obsd} \geq 2\sigma_c(I)$ were used in refinement. In the final

half of the structure at one time. The fluorenyl group and the potassium atom were varied together in one cycle and the atoms of the TMEDA molecule were varied in another.

The final positional and thermal parameters for the non-hydrogen atoms are contained in Tables I and II, respectively. Table III gives the hydrogen atom positions and thermal parameters.[9] Interatomic distances and angles are given in Tables IV and V.

Discussion

Molecular Structure of $C_{13}H_9K(N_2C_6H_{16})$. The structure of $C_{13}H_9K(N_2C_6H_{16})$, shown in Figure 1, was quite different from expected in that the TMEDA molecule is not bidentate. In the solid, there are infinite chains composed of alternating anions and cations, linked together by the amine ligands which are coordinated to the cations of neighboring chains. The bc

(8) R. F. Stewart, E. R. Davidson, and W. T. Simpson, *J. Chem. Phys.*, **42**, 3175 (1965).

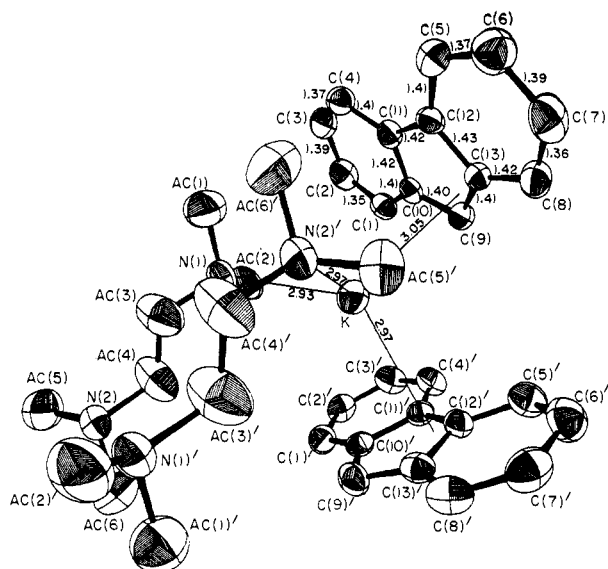(9) See paragraph at end of paper regarding supplementary material.

Figure 1. The molecular geometry of $C_{13}H_9K(N_2C_6H_{16})$.

Table III. Positional Parameters and Isotropic Thermal Parameters for the Hydrogen Atoms in $C_{13}H_9K(N_2C_6H_{16})$

Atom	x	y	z	B^a
H(1)	0.1564	0.3131	0.0977	5.12
H(2)	−0.0076	0.2405	−0.0490	3.73
H(3)	0.0492	0.1449	−0.1702	7.63
H(4)	0.2758	0.1192	−0.1287	4.07
H(5)	0.5683	0.1119	−0.0535	4.42
H(6)	0.8107	0.1357	0.0253	7.42
H(7)	0.8993	0.2284	0.1783	4.90
H(8)	0.7457	0.3039	0.2466	4.35
H(9)	0.4625	0.3371	0.2086	3.57
HA(11)	0.3366	−0.0207	0.1990	11.93
HA(12)	0.1627	−0.0192	0.1311	12.05
HA(13)	0.2717	0.0437	0.1194	12.42
HA(21)	0.1349	0.1294	0.3197	10.76
HA(22)	0.1413	0.1303	0.1845	9.98
HA(23)	0.0519	0.0650	0.2038	10.14
HA(31)	0.3422	−0.0504	0.3968	9.95
HA(32)	0.1581	−0.0412	0.3285	9.92
HA(41)	0.3451	0.0388	0.5149	9.66
HA(42)	0.1905	0.0341	0.4300	9.71
HA(51)	0.1546	−0.1336	0.4763	10.10
HA(52)	0.1875	−0.1353	0.6328	9.46
HA(53)	0.0985	−0.0771	0.6576	9.51
HA(61)	0.4036	0.0138	0.7209	9.92
HA(62)	0.2397	0.0087	0.6951	11.02
HA(63)	0.3455	−0.0604	0.7742	11.43

^{a} The form of the isotropic thermal parameter is $\exp[-B(\sin^2\theta/\lambda^2)]$.

projection of the contents of the unit cell illustrates the molecular network present in the crystal (Figure 2). The coordination sphere of the potassium atom is made up of two tertiary amines and two unsaturated organic groups instead of the coordination grouping of two tertiary amines and one unsaturated organic group found for the lithium atom in amine solvated unsaturated organolithium compounds.[2-4]

The fact that TMEDA does not effectively chelate a single potassium atom but acts as a bifunctional ligand to two potassium atoms is relevant to the aggregation properties of FlK–TMEDA in solution. The reason for the inability of TMEDA to chelate the potassium atom is not difficult to determine. The maximum radial extension of the nitrogen atom lone pair electrons
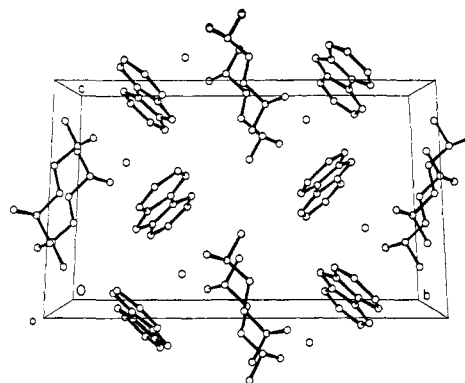

Figure 2. The bc projection of the unit cell of $C_{13}H_9K(N_2C_6H_{16})$.

Table IV. Interatomic Distances (Å) for the Non-Hydrogen Atoms in $C_{13}H_9K(N_2C_6H_{16})$

Atoms	Distance	Atoms	Distance
K–N(1)	2.928 (3)^a	C(7)–C(8)	1.358 (4)
K–N(2)'	2.965 (3)	C(8)–C(13)	1.419 (4)
K–C(9)	3.074 (2)	C(9)–C(10)	1.401 (4)
K–C(10)	3.350 (2)	C(9)–C(13)	1.410 (4)
K–C(13)	3.249 (2)	C(10)–C(11)	1.419 (4)
K–C(11)'	3.176 (2)	C(11)–C(12)	1.417 (4)
K–C(12)'	3.043 (2)	C(12)–C(13)	1.432 (4)
C(1)–C(2)	1.352 (4)	N(1)–AC(1)	1.452 (5)
C(1)–C(10)	1.409 (4)	N(1)–AC(2)	1.439 (4)
C(2)–C(3)	1.394 (5)	N(1)–AC(3)	1.448 (5)
C(3)–C(4)	1.370 (4)	AC(3)–AC(4)	1.367 (6)
C(4)–C(11)	1.410 (4)	N(2)–AC(4)	1.438 (5)
C(5)–C(12)	1.409 (4)	N(2)–AC(5)	1.439 (4)
C(5)–C(6)	1.368 (4)	N(2)–AC(6)	1.440 (4)
C(6)–C(7)	1.386 (4)		

^{a} Errors in the lattice parameters are included in the estimated standard deviations.

Table V. Bond Angles (deg) for the Non-Hydrogen Atoms in $C_{13}H_9K(N_2C_6H_{16})$

Atoms	Angle	Atoms	Angle
N(1)–K–N(2)'	90.4 (1)^a	C(10)–C(11)–C(12)	107.7 (3)
C(9)–K–C(12)'	86.3 (1)	C(4)–C(11)–C(12)	132.7 (3)
C(19)–K–C(11)'	86.4 (1)	C(11)–C(12)–C(13)	107.6 (3)
C(2)–C(1)–C(10)	119.6 (3)	C(11)–C(12)–C(5)	133.2 (3)
C(1)–C(2)–C(3)	122.8 (3)	C(5)–C(12)–C(13)	119.2 (3)
C(2)–C(3)–C(4)	118.9 (3)	C(9)–C(13)–C(12)	107.8 (3)
C(3)–C(4)–C(11)	120.4 (3)	C(8)–C(13)–C(9)	133.7 (3)
C(6)–C(5)–C(12)	120.0 (3)	C(8)–C(13)–C(12)	118.5 (3)
C(5)–C(6)–C(7)	120.5 (3)	AC(1)–N(1)–AC(2)	108.5 (3)
C(6)–C(7)–C(8)	121.8 (3)	AC(1)–N(1)–AC(3)	105.6 (3)
C(7)–C(8)–C(13)	119.8 (3)	AC(2)–N(1)–AC(3)	113.5 (3)
C(10)–C(9)–C(13)	108.4 (3)	N(1)–AC(3)–AC(4)	119.8 (4)
C(9)–C(10)–C(1)	132.8 (3)	N(2)–AC(4)–AC(3)	121.2 (5)
C(9)–C(10)–C(11)	108.6 (3)	AC(5)–N(2)–AC(6)	109.0 (3)
C(1)–C(10)–C(11)	118.6 (3)	AC(5)–N(2)–AC(4)	112.3 (3)
C(10)–C(11)–C(4)	119.6 (3)	AC(6)–N(2)–AC(4)	105.3 (3)

^{a} Errors in lattice parameters are included in the estimated standard deviations.

is expected to be coincident with the mean vector obtained by vectorically averaging the two nitrogen-methyl carbon atom vectors and the nitrogen–methylene carbon atom vector. A survey of ethylenediamine chelated metal complexes suggests that the N–N distance is relatively constant and about 2.9 ± 0.1 Å. The radial maxima of the lone pair orbitals of the two nitrogen atoms, therefore, make an angle of 85 ± 3° with each other (Figure 3). The effectiveness of the

TMEDA molecule as a bidentate chelating group for the potassium atom must be considerably less than for the lithium atom since the nitrogen atom lone pair electron density cannot be optimally directed toward the potassium atom. As a result, the basicity of the tertiary amine nitrogen atoms is much better utilized if the ligands act as monodentate bases. It is interesting that even though the compound was crystallized from a solution containing a large excess of TMEDA the coordination sphere of the potassium atom was increased not by adding one or two additional nitrogen atoms of a second TMEDA molecule but by sharing fluorenyl carbanions.

The specific orientation of the groups around the potassium cation is of considerable interest. A perpendicular line from the potassium atom to the five-membered ring plane of the fluorenyl group located 3.052 (1) Å away intersects the plane just inside the five-membered ring 0.39 Å to one side of C(9). A perpendicular line from the same potassium atom to the five-membered ring plane of a second fluorenyl group located 2.972 (1) Å away intersects the plane inside the five-membered ring 0.68 and 1.15 Å from C(12)' and C(11)', respectively. The angles formed by those carbon atoms nearest the potassium atom and the potassium atom itself, C(9)-K-C(11)' and C(9)-K-C(12)', are 86.43 (5) and 86.28 (6)°, respectively. The N(1)-K-N(2)' angle formed by the two amine nitrogen atoms and the potassium atom is 90.4 (1)°. This is to be compared with the N(1)-Li-N(2) angle in fluorenyllithium bisquinuclidine[3] of 123.7 (5)° and in benzyllithium triethylenediamine[2] of 118.6 (10)°. In all these cases, the amine nitrogen atoms are independent from each other relative to a given metal site. The distance between the potassium atom and the five-membered ring carbon atoms range from 3.043 (2) to 3.679 (2) Å with an average of 3.323 Å. This is in good agreement with the value of 3.30 Å predicted by the method of Johnson, et al.,[10] for a η^5-C_5H_5 group.

It is clear from the differences in the metal coordination spheres and the positions of the metal atoms with respect to the fluorenyl rings in the structures of the potassium and lithium fluorenyl systems that the directed valence model used to describe the fluorenyllithium bisquinuclidine structure does not apply to the potassium fluorenyl-TMEDA system. The valence orbitals of the potassium atom are more diffuse than the 2p orbitals of lithium, and the larger radius of the potassium atom makes it a poor polarizing group. Therefore, directed covalent interactions should be less important in organopotassium chemistry than in organolithium chemistry, and a purely electrostatic model can be used to explain to a relatively good approximation the observed configuration in the title compound. A calculation of the potential energy surface 2.0 Å above the plane of the carbanion as derived from the INDO calculated charge distribution for the fluorenyl carbanion indicates a potential energy minima just inside the C(9) position. The corresponding potential energy surface at 3.0 Å above the fluorenyl ring has a potential energy minima shifted toward the center of the five-membered ring. No attempts were made to minimize the potential energy surface with respect to two posi-

(10) C. Johnson, J. Toney, and G. D. Stucky, *J. Organometal. Chem.*, 40, C11 (1972).
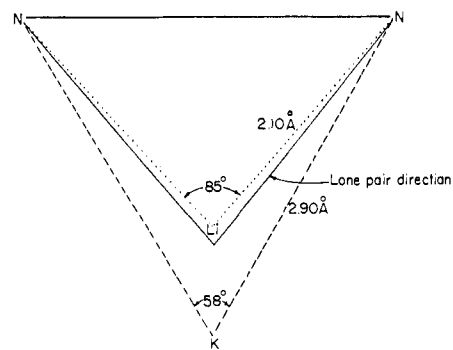

Figure 3. Hypothetical N-K-N angle for a potassium atom chelated to TMEDA compared to that observed for TMEDALi complexes. The direction of the lone pair electrons is obtained as the mean vector of the two N-CH$_3$ vectors and the N-CH$_2$ vector for each nitrogen atom.

tive point charges; however, the second potential minimum obtained with one positive point charge located 3.0 Å above the fluorenyl ring at a point 0.3 Å inside the C(9) position is just inside the C(11)-C(12) position on the other side of the ring. This is, in fact, close to what is observed, although the potassium atom is closer to C(13) (3.249 (2) Å) than C(10) (3.350 (2) Å) and closer to C(12) (3.043 (2) Å) than C(11) (3.176 (2) Å). Although absolute values obtained from the potential calculation are probably meaningless, it is interesting to note that differences between the calculated potential minimum positions and observed potassium positions represent less than 1.0 kcal.

An alternative electrostatic model which would emphasize a small covalent contribution to the bonding can be proposed. Hybridized potassium orbitals can be constructed using the potassium 4s, 4p, and 3d orbitals which have the proper geometry and symmetry for interacting with the HOMO of the two fluorenyl carbanions and the lone pairs on the amine nitrogens. An electrostatic model with such a covalent contribution can account for the observed C(9)-K-C(11'), C(9)-K-C(12'), and N(1)-K-N(2') angles of near 90°.

Steric effects may also be significant in the deviations noted above from the predicted electrostatic positions for the potassium atoms and in the particular geometry of the potassium coordination sphere. The methyl groups on the amine nitrogen atoms are on the order of 3.85 Å from several carbon atoms in the fluorenyl groups, and the sum of the van der Waals radii for a methyl group and an aromatic ring is 3.85 Å. Some of these fluorenyl groups belong to the same potassium coordination sphere as the nitrogen atoms to which the methyl groups are bonded and others belong to different coordination spheres. The closest carbon-carbon atom distance between adjacent fluorenyl groups is also about 3.85 Å. A comparison of the fluorenyl ring bond lengths in fluorenyllithium bisquinuclidine[3] and fluorenylpotassium tetramethylethylenediamine and the π Hückel bond order bond lengths is given in Figure 4. The observed fluorenyl carbanion bond lengths are averaged over the molecular symmetry of the isolated carbanion and compared with the Hückel bond order bond lengths in Table VI. The agreement is quite good.

The fluorenyl carbanion deviates to some extent from planarity (plane 1, Table VII). The inner five-mem-
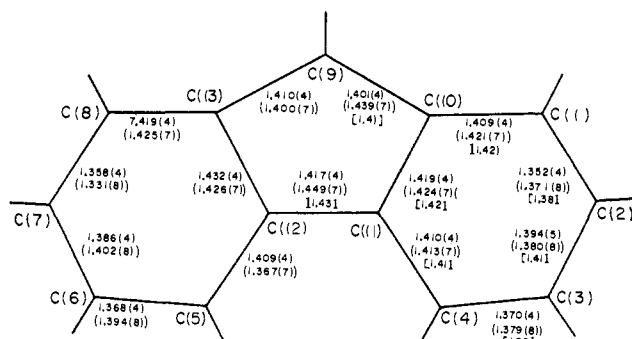
Figure 4. Comparison of fluorenyl carbanion bond lengths. Numbers without parentheses or brackets are from this investigation for $C_{13}H_9K(N_2C_6H_{16})$, numbers in parentheses are for $C_{13}H_9Li(NC_7H_{13})_2$, and numbers in brackets are Hückel π bond order distances.

Table VI. Comparison of Symmetry Averaged Bond Lengths for Fluorenyllithium Bisquinuclidine and Fluorenylpotassium–TMEDA with the Hückel π Bond Order Bond Lengths

Bond	Obsd average (Å) bond length	Bond order bond length (Å)
C(1)–C(10)	1.418 (3)	1.42
C(9)–C(10)	1.413 (9)	1.41
C(1)–C(2)	1.353 (8)	1.38
C(2)–C(3)	1.391 (5)	1.41
C(3)–C(4)	1.378 (6)	1.39
C(4)–C(11)	1.400 (10)	1.41
C(11)–C(12)	1.433 (10)	1.43
C(10)–C(11)	1.425 (5)	1.42

bered ring of the fluorenyl carbanion is planar within experimental error, but the two outer six-membered rings are nonplanar (plane 4, plane 2, plane 3; Table VII). The benzyl fragments show an even greater deviation from planarity (plane 5, plane 6; Table VII). The nonplanarity of the benzyl fragments is due to a large extent to the deviation of C(9) from the planes of the six-membered rings (plane 2, plane 3; Table VII). Considering these planes, C(9) is 0.042 (3) and 0.061 (3) Å out of plane 2 and plane 3, respectively. This is in contrast to the molecular structure of fluorenyllithium bisquinuclidine in which C(9) is 0.042 (6) Å out of the plane of only one of the six-membered rings. The nonplanarity of the benzyl fragments as well as the entire fluorenyl carbanion for FlK–TMEDA can also be explained by the fact that the two six-membered rings are tipped toward each other, 1.3 and 1.9°, respectively, from the plane of the five-membered ring.

Solid State Spectroscopic Results. The interaction of the fluorenyl anion with the alkali metal cation in solution has been extensively investigated by spectroscopic and conductance studies.[1,11,12] Much of the interest in these compounds has centered on the nature of the ion pairs formed in various solvents.

Chan and Smid[11] interpret the results of their ultraviolet and visible absorption spectra of carbanions in terms of contact and solvent-separated ion-pair formation. This concept is undoubtedly essentially correct; however, as pointed out in the introductory section, the exact nature of the fluorenyl–alkali metal "contact" and "solvent separated" (or "loose") ion pairs is not yet clear. For example, the formation of solvent sep-

(11) L. L. Chan and J. Smid, *J. Amer. Chem. Soc.*, **90**, 4654 (1968).
(12) T. Ellingsen and J. Smid, *J. Phys. Chem.*, **73**, 2712 (1969).

arated 9-alkyl substituted fluorenyllithium ion pairs is much more pronounced than for unsubstituted fluorenyllithium.[13] This is not observed for sodium salts so that steric effects do not seem to be an important factor. The geometry of an allylic fluorenyllithium complex as observed for fluorenyllithium bisquinuclidine would, however, be greatly affected by 9-methyl substitution and could explain the above effect. As noted above, sodium salts are not expected to adopt this geometry.

Recent results have shown that in "low-polarity" solvents, fluorenyllithium complexes are aggregated.[14] The difference between "solvent separated" and "contact" could conceivably be due to a difference of aggregation. What, in fact, is the effect on the absorption spectrum of a fluorenyl carbanion when the number of metal atoms with which it associates is changed from one to two or more? It is also not clear what effect a change in the solvation number of the lithium atom from two to three would have upon the absorption spectrum. Since, in contrast to solution studies, the solid state structural data give one the distinct advantage that one knows precisely the species with which one is dealing, it seemed profitable to examine the spectroscopic properties of the fluorenyl carbanion with a variety of counterions in the solid state (Table VIII).

The value of λ_{max} for fluorenyllithium (contact ion pair) in solution ranges from 346 nm for dioxane to 349 nm for THF. The solid state values of λ_{max} for fluorenyllithium complexes vary over a much wider range, 345 nm for FlLi·2THF to 360 nm for FlLi·HMPA. The value of λ_{max} for fluorenylpotassium (contact ion pair) in THF is 362 nm while in the solid state the TMEDA complex has a value of λ_{max} of 380 nm. This bathochromic shift is even larger than that for the solvent separated ion pair which has a value of λ_{max} of 373 nm. The value of λ_{max} for $Fl(n\text{-Bu})_4N$ (contact ion pair) in THF is 368 nm while in the solid state the value of λ_{max} for $Fl(n\text{-Pr})_4N$ is 374 nm. The free ion value of λ_{max} for the fluorenyl carbanion in solution is also 374 nm.

A shift in the energy of the $\pi \rightarrow \pi^*$ transitions is a result of a change in the stabilization of the ground state (HOMO) relative to the stabilization of the excited state of the carbanion. Simple MO calculations[15] indicate the charge moves from the benzylic position out onto the rings in the excited state. There are two ways in which the relative stabilization of the ground state and excited state can be affected so as to cause a bathochromic shift in the transition energy. If the metal ion becomes more highly solvated or the basicity of the solvent is increased, the interaction between the cation and the benzylic region of the fluorenyl carbanion will decrease and the difference between the stabilization of the ground state relative to the excited state will decrease. If the fluorenyl carbanion in a crystal lattice can interact with more than one metal ion such that the interaction is more general and not specifically limited to the benzylic region of the carbanion, the difference

(13) M. M. Exner, R. Waack, and E. C. Steiner, Abstracts, 161st National Meeting of the American Chemical Society, Los Angeles, Calif., 1971, No. ORGN-184.
(14) T. E. Hogen-Esch and J. Smid, *J. Amer. Chem. Soc.*, **89**, 2764 (1967).
(15) A. Streitwieser, Jr., and J. I. Brauman, "Supplemental Tables of Molecular Orbital Calculations," Pergamon Press, New York, N. Y., 1970.

Table VII. Best Weighted Least-Squares Planes for $C_{13}H_9K(N_2C_6H_{16})$

Plane	Atoms in plane	Equation of plane[a,b]
1	C(1),C(2),C(3),C(4),C(5),C(6), C(7),C(8),C(9),C(10),C(11), C(12),C(13)	$0.2310x + 0.6424y - 0.7307z - 3.0748 = 0$
2	C(1),C(2),C(3),C(4),C(10),C(11)	$0.2464x + 0.6438y - 0.7244z - 3.1187 = 0$
3	C(5),C(6),C(7),C(8),C(12),C(13)	$0.2086x + 0.6435y - 0.7369z - 2.9217 = 0$
4	C(9),C(10),C(11),C(12),C(13)	$0.2375x + 0.6301y - 0.7393z - 3.0301 = 0$
5	C(1),C(2),C(3),C(4),C(9),C(10), C(11)	$0.2413x + 0.6395y - 0.7299z - 3.0939 = 0$
6	C(5),C(6),C(7),C(8),C(9),C(12), C(13)	$0.2176x + 0.6370y - 0.7398z - 2.9595 = 0$

Atom	Deviations of Atoms from Planes (Å)					
	Plane 1	Plane 2	Plane 3	Plane 4	Plane 5	Plane 6
C(1)	0.002 (4)	−0.006 (4)			0.013 (4)	
C(2)	0.021 (4)	−0.005 (4)			−0.000 (4)	
C(3)	0.031 (4)	0.008 (4)			0.018 (4)	
C(4)	0.001 (3)	−0.000 (3)			0.003 (3)	
C(5)	−0.030 (3)		−0.021 (3)			−0.017 (3)
C(6)	0.055 (4)		0.030 (4)			0.044 (4)
C(7)	0.026 (4)		−0.008 (4)			−0.001 (4)
C(8)	−0.001 (3)		−0.008 (4)			−0.001 (4)
C(9)	0.0081 (3)	0.042 (3)	0.061 (3)	0.002 (3)	0.016 (3)	0.024 (3)
C(10)	−0.003 (3)	0.010 (3)		−0.002 (3)	−0.004 (3)	
C(11)	−0.024 (3)	−0.007 (3)		0.001 (3)	−0.016 (3)	
C(12)	−0.031 (3)		0.003 (3)	0.003 (3)		−0.010 (3)
C(13)	−0.012 (3)		0.011 (3)	−0.001 (3)		−0.008 (3)
K	−3.051 (1)	−3.015 (1)	−3.001 (1)	−3.052 (1)	−3.040 (1)	−3.034 (1)
K′	2.9501 (1)	2.985 (1)	2.993 (1)	2.972 (1)	2.967 (1)	2.974 (1)

The dihedral angle between planes 2 and 3 is 2.4°
The dihedral angle between planes 5 and 6 is 1.5°
The dihedral angle between planes 2 and 4 is 1.3°
The dihedral angle between planes 3 and 4 is 1.9°

[a] The orthogonal unit cell vectors x, y, and z are related to the monoclinic vectors a, b, and c as follows: $(x,y,z) = (a + c \cos \beta, b, c \sin \beta)$. [b] The weight of each atom is inversely proportional to the mean variance of the positional parameters for that atom.

Table VIII. Solid State Uv–Visible Spectra of Various Fluorenyl Salts (nm)

	ν_1	ν_2	ν_3	ν_4[a]	ν_5[a]	ν_6[a]
FlLi		355		420	460	490
FlLi–PMDTA[b]		357		400	450	480
FlLi–TMEDA[c]		345		410	433	460
FlLi–HMPA[d]		360		420	453	480
FlLi–2THF[e]		345		400	440	470
FlK–TMEDA[c]	320		380	460	490	515
Fl(n-Pr)$_4$N[f]	320		374	430	455	487

[a] Very broad bands. [b] Pentamethyldiethylenetriamine. [c] Tetramethylethylenediamine. [d] Hexamethylphosphoramide. [e] Tetrahydrofuran. [f] Tetra-n-propylammonium cation.

between the stabilization of the two states will also decrease.

Using the above concept, the bathochromic shifts observed in the solid-state spectra can be explained. For FlLi–TMEDA and FlLi–2THF, we find very little change in λ_{max} from that found in solution since their structures undoubtedly are similar to that reported for fluorenyllithium bisquinuclidine in which the lithium atom occupies an allylic position with respect to the fluorenyl ring. Because in the solid the contact ion pairs are probably "tighter," one actually sees a slight hypsochromic shift. In FlLi–PMDTA, we see a substantial bathochromic shift since the metal is now probably coordinated to three amine nitrogens. The bathochromic shift observed for the unsolvated fluorenyllithium is most likely caused by the second reason discussed previously. Since the metal ion is completely unsolvated, a given carbanion will be in close prox-

imity to several metal ions in the lattice, thus reducing the energy difference of the ground and excited states. The close contact of the fluorenyl carbanion to more than one potassium metal ion also explains the very large bathochromic shift observed in FlK–TMEDA. Each carbanion is closely associated with two potassium atoms and, in addition, contact ion pairs are only van der Waals distances apart from each other. The effects of a crystal lattice on contact ion pairs are also observed in the bathochromic shift of 6 nm observed for Fl(n-Pr)$_4$N$^+$ in going from solution to the solid state. Because the charge separation is large initially, the lattice environment has a reduced effect. The bathochromic shift found for FlLi–HMPA is probably a result of both effects discussed previously. The strong solvating properties of HMPA which reduces the anion–cation interaction plus the fact that monosolvation would sterically allow increased interaction between ion pairs accounts for the magnitude of the shift observed.

In addition to solvent effects, the spatial relationship between ion pairs can have a profound effect on the $\pi \rightarrow \pi^*$ transition energy of the fluorenyl carbanion. As shown, close contact between ion pairs can produce bathochromic shifts equal to those caused by complete solvation of the metal ion. If the possibility of having aggregated species in solution exists, considerable care must be exercised in the interpretation of the 370-nm band of the fluorenyl carbanion since an absorption in this region does not necessarily reflect the presence of "loose" or solvent separated ion pairs.

Ab Initio SCF Calculations of the Acidity of Distorted Ethanes and Ethylenes[1]

Andrew Streitwieser, Jr.,* **Peter H. Owens,[2a]** **Richard A. Wolf,[2b]** **and James E. Williams, Jr.**

Contribution from the Department of Chemistry, University of California, Berkeley, California 94720. Received October 3, 1973

Abstract: *Ab initio* SCF calculations are presented for ethane, ethyl anion, ethylene, and vinyl anion in which the β H–C–H angles are distorted from their normal values. The results provide a simple model for the effect of small or strained rings on the acidity of adjacent bonds. The results are also consistent with changes in the s character of bonds as determined either by overlap populations or by localized molecular orbitals.

R ecent kinetic acidity studies have demonstrated a general effect of ring strain in enhancing the acidity of an adjacent C–H bond. The 1 position of biphenylene, adjacent to a four-membered ring, is 79 times more reactive toward lithium cyclohexylamide than is the 2 hydrogen.[3] Even in the aryl positions of triptycene, the 1 position, adjacent to the strained bridgehead, is 7.5 times more reactive than the 2 hydrogen in kinetic acidity toward cesium cyclohexylamide. The generality that a hydrogen adjacent to a small or strained ring has enhanced acidity extends to other kinds of systems as well; for example, cyclopropylamine has reduced basicity compared to alkylamines.[4] The explanation has been advanced that the bond orbital exocyclic to a small ring has higher s character and, hence, greater electronegativity that enhances the acidity of an adjacent bond to hydrogen.[3] However, attempts to model the effect by appropriate semiempirical SCF calculations (CNDO, INDO, MINDO) have not given an adequate accounting of this phenomenon.[5] Since semiempirical MO methods are generally parameterized with nonstrained systems, this result is neither surprising nor useful. In the present study we demonstrate that *ab initio* SCF methods, even at the minimum basis set level, provide a satisfying theoretical model that confirms the earlier interpretation. The calculations were made on ethanes and ethylenes in which the β CH_3 and CH_2 groups, respec-

tively, were given varying HCH bond angles and on the corresponding carbanions generated by removing a proton from the α carbon. In this type of approach the calculated absolute proton affinity of the carbanions is of less significance than the changes produced by the β HCH angle perturbations.

Ethane and Ethyl Anion

Calculations on this system used the STO-4G basis set[6] with optimized geometry and exponents. The isotropic sp (iso/sp)[7] basis was used in which the 2s and 2p exponents are constrained to be equal. All calculations were made with the modified IBMOLIV program described previously.[7] The values obtained are summarized in Table I. Ethane has been examined

Table I. Optimized Exponents and Geometry of Ethane and Ethyl Anion

	Ethane[a]	Ethyl anion
C (1s)	5.67	(5.67)[a]
C (2s, 2p) β	1.75	1.775
C (2s, 2p) α	1.75	1.551
H (1s) β	1.17	1.117
H (1s) α	1.17	1.111
r(CC), Å	1.524	1.551
r(CH) β, Å	1.094	1.128,[b] 1.126[c]
r(CH) α, Å	1.094	1.179[d]
Energy, au	−78.8708	−78.0688

[a] Assumed value; ethane exponents from ref 6. [b] Anti to lone pair; $C_α–C_β–H_{anti}$ = 116.0°. [c] Gauche to lone pair; $H_{gauche}–C–H_{gauche}$ = 106.3°; $C_α–C_β–H_{gauche}$ = 111.0°. [d] H–$C_α$–H = 99.6°; $C_β–C_α$–H = 107.0°

previously by the STO-NG method;[6] our optimized geometry and orbital exponents as determined by

(1) Acknowledgment is made to National Science Foundation, Grant no. 29383, and the donors of the Petroleum Research Fund, administered by the American Chemical Society, for partial support of this research. Additional computer time was donated by the Computer Center, University of California, Berkeley.

(2) (a) U. S. Public Health Predoctoral Fellow, 1968–1970; (b) National Institutes of Health Postdoctoral Fellow, 1968–1969.

(3) A. Streitwieser, Jr., G. R. Ziegler, P. C. Mowery, A. Lewis, and R. G. Lawler, *J. Amer. Chem. Soc.*, **90**, 1357 (1968).

(4) J. D. Roberts and V. C. Chambers, *J. Amer. Chem. Soc.*, **73**, 5030 (1951).

(5) P. C. Mowery, Dissertation, University of California, Berkeley, 1971.

(6) W. J. Hehre, F. R. Stewart, and J. A. Pople, *J. Chem. Phys.*, **51**, 2657 (1969).

(7) P. H. Owens and A. Streitwieser, Jr., *Tetrahedron*, **27**, 4471 (1971).